A Small-Angle X-ray Scattering Study of the Phase Behavior of Diblock Copolymer/Homopolymer Blends

Jeffrey Bodycomb,[†,‡] Daisuke Yamaguchi,[§] and Takeji Hashimoto*[,†,§]

Hashimoto Polymer Phasing Project, ERATO, JST, Kyoto, Japan; and Department of Polymer Chemistry, Graduate School of Engineering, Kyoto University, Kyoto 606-8501, Japan

Received October 26, 1999; Revised Manuscript Received April 27, 2000

ABSTRACT: The order−disorder transition (ODT), microdomain morphology, and phase behavior in mixtures of polystyrene-*block*-polyisoprene (SI) diblock blended with homopolystyrene (HPS) were investigated. SI with a total molecular weight of 2.0×10^4 and volume fraction of polystyrene (PS) of 0.51 (designated SI-11/9) was blended with a homopolystyrene of molecular weight 6.1×10^3 (designated S-6). Binary mixtures of diblock copolymer and homopolymer were prepared by solvent casting. The ODT was *quantitatively* identified using the discontinuity observed in a plot of the reciprocal of the peak small-angle X-ray scattering (SAXS) intensity, I_m^{-1}, as a function of the reciprocal of the absolute temperature, $1/T$, except for the mixtures showing the disordered sphere morphology for which we determined the temperature of the demicellization/micellization transition (DMT) instead of the ODT by the disappearance of the form factor peak with increasing temperature. We systematically measured the ODT or DMT temperature as a function of the volume fraction of homopolymer. SAXS data were also used to investigate the microdomain structure of the blends. Furthermore, for two blends of SI-11/9 and S-6 with volume fractions of SI of 0.77 and 0.71, we observed an order−order transition (OOT) from a cylindrical structure to a gyroid structure on heating above 110 °C for the 0.77 volume fraction blend and 100 °C for the 0.71 volume fraction blend. However, the reverse transition from gyroid to cylinder on cooling the 0.77 volume fraction blend to below 110 °C was not observed even after annealing at temperatures below 110 °C for more than 10 h, possibly due to kinetic effects. Slow cooling (2−3 h) of the blend from the disordered state led to the gyroid structure even below 110 °C, while the low-temperature cylindrical phase could only be accessed by fast cooling (1.5 h) from the disordered state. Experimentally determined ODTs or DMTs are compared with predictions based on mean field theory. The predicted effect of homopolymer concentration on the ODT or DMT temperature was quantitatively consistent with that found experimentally. The phase diagram of the diblock copolymer/homopolymer blend was found to show the same complexity as and similar features to phase diagrams of pure diblock copolymers.

1. Introduction

The phase behavior of diblock copolymers and their blends, either with homopolymers or other diblock copolymers, is an interesting topic with respect to microphase separation behavior.[1,2] In this paper, we examine the behavior of blends of a diblock copolymer with a homopolymer as a function of blend composition and temperature to obtain an experimental phase diagram for a diblock copolymer/homopolymer blend. Although this research topic is not new, we believe we still lack systematic and quantitative studies of effects of homopolymer addition on phase diagrams: this is partly because quantitative and unequivocal determination of the ODTs for the blend systems have not necessarily been attained in previous works as will be detailed below and partly because the studies involve a huge parameter space, with parameters such as molecular weight and composition of diblock copolymers, molecular weight of homopolymers, composition of block copolymers or homopolymers, temperature, and pressure. Thus, the state of the art of this field is still very immature, hence deserving a collection of more reliable and quantitative experimental data for a better understanding of this scientifically and technologically important field. The present work which can naturally explore only a small part of this parameter space (homopolymer composition and temperature) is aimed to add a contribution to this field.

Mean-field theory has proven useful in interpreting the behavior of block copolymer systems. It predicts that the scattered intensity $I(q)$ at a scattering vector $q = (4\pi/\lambda)\sin(\theta/2)$ (λ is the wavelength of the X-ray beam, and θ is the scattering angle) from disordered materials is given by the relation $[I(q)]^{-1} \sim F(q) - 2\chi$, where $F(q)$ is a function that depends on the volume fraction of each blend component, radius of gyration of the block copolymer, $R_{g,b}$, the homopolymer radius of gyration, $R_{g,h}$, and the volume fraction of each block in the block copolymer.[3,4] χ is Flory's segmental interaction parameter. $F(q)$ has a minimum, and hence $I(q)$ has a maximum denoted I_m at a particular value of q, q_m. The value of χ changes with temperature, T, and its behavior is usually described by an equation of the form $\chi = A + B/T$ where A and B are constants and T is the absolute temperature. Under the condition $\chi = F(q_m)/2$ the value of $[I(q_m)]^{-1}$ is zero and the value of $I(q_m)$ diverges, which marks the mean-field spinodal point of the system for microphase separation for $q_m \neq 0$ and for the macrophase transition for $q_m = 0$. In the mean-field disordered state, the value of I_m^{-1} changes linearly with $1/T$ due to the $1/T$ dependence of χ. Deviations from this linear behavior were previously interpreted as the order−disorder transition (ODT).[4−10] Several experimental studies have used these criteria to examine the ODT in mixtures of block copolymer and homopolymer.[7,9−12]

* To whom correspondence should be addressed.
† ERATO, JST.
‡ Current address: Polymer Dynamics, Inc. PO Box 4400. 2200 South 12th Street, Allentown, PA 18105-4400.
§ Kyoto University.

10.1021/ma9917996 CCC: $19.00
Published on Web 06/17/2000

However, it has recently been shown theoretically[13] and experimentally[14−30] that this view is incomplete. The mean-field description of Leibler[4] does not take into account the effect of thermal noise (fluctuations).[4,13] A correction for fluctuation effects has been calculated by Fredrickson−Helfand (FRH), though it is only rigorously applicable to high molecular weight copolymers.[13] The FRH theory predicts a deviation from linear behavior in the plot of I_m^{-1} vs $1/T$ even in the disordered state, especially near the ODT. Furthermore, a discontinuity in the plot of I_m^{-1} vs $1/T$ at the ODT was predicted. Experimentally, it has been shown that pure diblocks show the effects of thermal fluctuations in the form of nonlinearity in the plot of I_m^{-1} vs $1/T$ at temperatures above the ODT temperature and more dramatically, a discontinuity in the plot of I_m^{-1} vs $1/T$ or a plot of σ_q^2, the square of the half-width at the half-maximum of the first-order scattering peak, vs $1/T$[14−20] at the ODT.

We naturally wonder if this new criterion for the determination of the ODT of pure block copolymers is also valid for blends of block copolymers and the corresponding homopolymers. Though it may be likely, it must be experimentally proven. In fact recently, we found that the new criterion applies not only to pure diblock copolymer but also to blends of diblock copolymers with homopolymers[21] and blends of two diblock copolymers.[21,22] Thus, we can now unequivocally determine the ODTs for blends of a diblock copolymer and a homopolymer. In this work we aimed to study quantitatively and systematically effects of homopolymer addition on the ODT with the new criterion. This is one of new features of the present work, since the ODTs of the blends have not yet been studied with the new criterion.

In blends of a polystyrene-based block copolymer and homopolystyrene, the microdomain structure in the ordered state depends on the volume fraction of polystyrene (PS) in the system (Φ_{PS}). Two summaries appear in the literature identifying the effect of the overall volume fraction of PS on microdomain structure.[23,24] The results of these two compilations nearly match. Blends with $0.32 < \Phi_{PS} < 0.61$ are expected to show lamella structure. For $0.61 < \Phi_{PS} < 0.68$ a bicontinuous structure is expected, for $0.68 < \Phi_{PS} < 0.77$, a cylindrical structure is expected, and for $\Phi_{PS} > 0.77$, a spherical structure is expected. Both of these reports presumed that the bicontinuous structure was OBDD. However, more recent results reveal that the observed bicontinuous structure is likely a gyroid structure.[25,26] Thus, the gyroid structure in blends of the diblock copolymer and the homopolymer deserves further studies. We focused on this point as well, which is another new feature of the present work.

To examine the effect of homopolymer composition on the ODT, we systematically varied the homopolymer composition. Since we used the newer criterion for the ODT, we expect that these results will be important in critically testing ideas concerning the behavior of diblock copolymer/homopolymer blends. Furthermore, the results on morphology variations with the composition including the gyroid morphology highlight the similarities and differences between pure diblock copolymers and their blends with homopolymers. Although the similarities are intuitively expected, this intution needs to be confirmed experimentally for basic understanding of the phase diagrams of the block copolymer/homopolymer blends.

Table 1. Characteristics of Polymers Used in This Study

specimen code	M_n[a]	M_w/M_n[a]	vol fract PS[b]	N_{eff}[b]
SI-11/9	1.96×10^4	<1.05	0.51	232
S-6	6.1×10^3	<1.05	1 (homopolymer)	69

[a] By GPC. [b] Value estimated by using[58] $\rho_{PS} = 1.052$ g/cm^3 and $\rho_{PI} = 0.925$ g/cm^3.

2. Experimental Methods

Diblock copolymers, polystyrene-*block*-polyisoprene (SI), were synthesized by living anionic polymerization with *sec*-butyllithium as an initiator and cyclohexane as a solvent and characterized by GPC. PS homopolymer was obtained from Tosoh Corporation with a number-average molecular weight of 6.1×10^3 as measured by GPC. Polymer characteristics are tabulated in Table 1 and designated according to the scheme presented by Winey et al.[24] Film samples were prepared by making a solution of 5 wt % polymer with a small amount (<1%) of antioxidant (Irganox 1010; Ciba-Geigy Corp.) in toluene, then filtering with a 0.5 μm Teflon filter, and slowly evaporating the solvent. Finally, the last of the solvent was removed in a vacuum oven at 150 °C for at least 10 h.

Temperature-dependent small-angle X-ray-scattering, SAXS, was measured in situ with a SAXS apparatus described elsewhere, except for the replacement of the X-ray generator with a new one (MAC Sciences M18X HF operated at 16 kW) for some experiments.[27−29] All measurements were conducted with the sample cell placed in an evacuated chamber to reduce thermal degradation. At each measuring temperature the samples were held for about 45 min and measured for about 1 h. SAXS profiles were desmeared for slit-width and slit-height smearing and were corrected for air scattering and absorption.[28] Our experimental procedure was to set the sample into the X-ray instrument and then measure the ODT while cooling, thus obtaining the approximate ODT temperature for the next, time-consuming step: high-temperature resolution experiments. In this step, we measured the scattering while raising the temperature in small steps to determine the ODT temperature.

TEM samples were prepared by cryoultramicrotomy at −90 °C, below the glass transition of PI ($T_g = -68$ °C) in order to preserve the structure of the sample, with a Reichert Ultracut E low-temperature sectioning system. A Hitachi H-600 transmission electron microscope operated at 100 kV was used to obtain micrographs of the specimens stained with osmium tetroxide. Osmium tetroxide is a selective stain for PI, leaving the PS domains of the sample bright and the PI domains dark under the TEM observation.

Error bars in this work, when given, correspond to 95% confidence intervals for the parameters presented unless noted otherwise. The first-order scattering peak from the block copolymer and homopolymer systems to be treated here is generally too sharp compared with the width of the slit weighting function of the conventional SAXS apparatus used here. In this case, desmearing of the smeared scattering profile is generally an ill-posed problem. When this difficulty is encountered, we avoid it as follows. We assume that the desmeared (true) scattering profile is a Gaussian or Lorentzian function with peak intensity I_m and a full width at half-maximum $2\sigma_q$. This function was smeared with the measured slit-width and slit-heigh weighting functions to obtain a smeared Gaussian or Lorentzian function. The smeared (measured) scattering function was then best fit with the smeared Gaussian or Lorentzian function. The best fit yielded the value of I_m and σ_q. Their error bars were estimated using usual propagation of error techniques.

3. Results

3.1. ODT and D Measurement. The first point in understanding the phase behavior of these blends is the criterion for identifying the ODT. Recent work on pure diblock copolymers[15−20] and blends of diblock copolymer

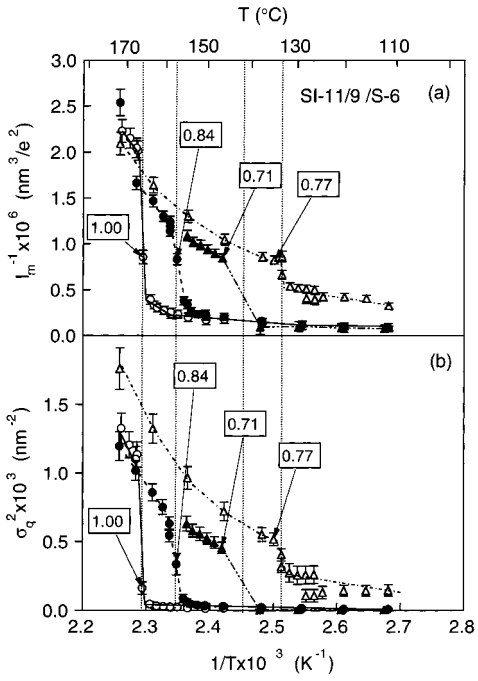

Figure 1. Plot of (a) I_m^{-1} vs $1/T$ and (b) σ_q^2 vs $1/T$ for pure SI-11/9 (○) and SI-11/9/S-6 blends with compositions 0.84/0.16 (v/v) (●); 0.77/0.23 (v/v) (△); and 0.71/0.29 (v/v) (▲). Vertical dotted lines indicate the ODT. Lines through points are to guide the eye.

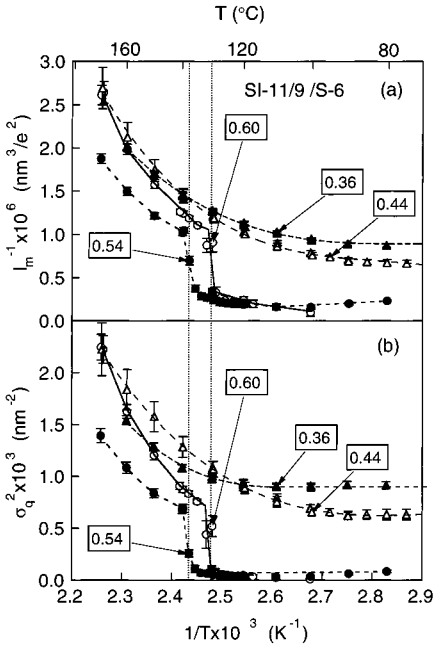

Figure 2. Plot of (a) I_m^{-1} vs $1/T$ and (b) σ_q^2 vs $1/T$ of SI-11/9/S-6 blends with compositions 0.60/0.40 (v/v) (○), 0.54/0.66 (v/v) (●), 0.44/0.56 (v/v) (△), and 0.36/0.64 (v/v) (▲). Vertical dotted lines indicate the ODT. Lines through points are to guide the eye.

with either homopolymers or other diblock copolymers,[21,22] as well as theoretical work,[30] has shown that the ODT is better characterized by a discontinuity in a plot of I_m^{-1} or σ_q^2 vs $1/T$ rather than a deviation from linear behavior in I_m^{-1} or σ_q^2 vs $1/T$.

In all of the blends discussed here, there is no upturn in the scattered intensity at low scattering vectors with decreasing q as $q \rightarrow 0$, and therefore, it is clear that there is no macrophase separation in this sample.[31] From the first-order scattering peak, we obtain three parameters characterizing the blend of SI and PS at a particular temperature: I_m, σ_q^2, and q_m. The value q_m gives either the dominant mode of the concentration fluctuations for the disordered state or the domain spacing of the system for the ordered state. Either of these lengths is expressed by the value $D = 2\pi/q_m$. The behavior of the values of I_m and σ_q^2 as a function of $1/T$ can be used to identify the ODT temperature.

To view the effect of temperature on I_m and σ_q for a blend system, we show a plot of (a) I_m^{-1} vs $1/T$ and (b) σ_q^2 vs $1/T$ for the diblock as well as its blends with PS (S-6) having volume fractions of the diblock of 1.00, 0.84, 0.77, and 0.71 in Figure 1. Here the data for only the heating process were shown in the figure, though the data generally showed hysteresis. An ODT can be clearly discerned from the discontinuity in either the I_m^{-1} or σ_q^2 values plotted against $1/T$ as found in the case of pure block copolymers. The vertical dashed lines are to indicate the discontinuity for each specimen and facilitate comparison of the I_m^{-1} and σ_q^2 data. While σ_q^2 is not independent of I_m^{-1}, it is independent of the absolute scattered intensity measurement and thus serves as a useful check for the I_m^{-1} data.

As for Figure 1, following observations are worth noting. For the blend compositions with a lot of diblock, that is, pure diblock and 0.84 volume fraction of diblock, the curves at $T > T_{ODT}$ seem linear with $1/T$, but this is due to a lack of data at temperatures above the ODT temperature. To avoid degradation, we did not heat the samples over 200 °C, and since the ODT temperature of some samples was quite high, it was impossible to obtain a reasonable number of well-spaced data points for examining the curvature of the plot above ODT. However, where more data are available at higher volume fractions of S-6, which give a lower ODT temperature, and therefore a greater range of accessible temperatures above the ODT temperature, we see that the plot of I_m^{-1} vs $1/T$ is indeed curved as predicted by fluctuation calculations.[13,30]

Furthermore, for the 0.77 volume fraction blend, the discontinuity marking the ODT is less pronounced. The weaker scattering (higher value of I_m^{-1}) and broader first-order scattering peak (higher value of σ_q^2) in the ordered state may be due to the fact that the sample does not order well. However, we are unsure if this is a result of the thermal history (annealing) of the sample or due to some difference in the ordering process of the blend. Note the relatively large error bars for values of I_m^{-1} and σ_q^2, about 10% or more of the measured values of I_m^{-1} or 25% of the measured values of σ_q^2 for all of the ordered samples studied here, including the 0.77 volume fraction blend. Note also that the blends with volume fractions of SI-11/9 of 0.77 and 0.71 can undergo an order−order transition (OOT) as well, depending on thermal history, as will be discussed later.

Two of the blends shown in Figure 2, 0.54/0.46 v/v and 0.60/0.40 v/v, have cylindrical structure. These blend compositions show the typical discontinuity in I_m^{-1} and σ_q^2 vs $1/T$, indicating the ODT. Also, above the ODT temperature, curvature in I_m^{-1} and σ_q^2 vs $1/T$ is quite apparent, again indicating strong fluctuation effects.[13,14,19]

For the I_m^{-1} and σ_q^2 plots of blends with 0.36 and 0.44 volume fraction of diblock shown in Figure 2, no discontinuity is observed. These blends form spherical microdomains composed of PI in a matrix of PS. However, as will be discussed later, spherical micro-

domains with only short-range liquidlike order (defined hereafter as "disordered spheres") form at a sufficiently low temperature, but no ordered lattice is formed. Rather than an ODT, we observe a pseudo-phase transition called a DMT (demicellization/micellization transition)[32] from a disordered phase with thermal composition fluctuations to spherical domains with liquidlike order with decreasing temperature. Since the samples do not order on a lattice, the lack of a discontinuity in I_m^{-1} vs $1/T$ is due to the fact the lattice ordering temperature is not accessible in the temperature range studied, because the polystyrene matrix phase vitrified at a temperature higher than the temperature below which lattice ordering occurs.

To discern whether the discontinuity, observed on the plot of I_m^{-1} or σ_q^2 vs $1/T$ for the blend specimens containing 0.84, 0.77, 0.71, 0.60, and 0.54 volume fractions of diblock (see Figures 1 and 2), in fact corresponds to the temperature of the ODT or the lattice disordering transition (LDT) or the lattice disordering/ordering transition (LDOT) as proposed by Sakamoto et al.[33−35] and Han et al.,[32] the overall scattering curves were carefully inspected. We noted that the scattering curves from the samples at temperatures above the discontinuity temperature had a different shape than the curves below the discontinuity temperature. That is, the region showing q^{-4} behavior indicating the presence of a sharp interface was not apparent at temperatures above the temperature of the discontinuity in I_m^{-1} or σ_q^2 vs $1/T$, but was apparent at temperatures below those at which the discontinuity is observed. In addition, the entire shape of the X-ray scattering curves as a function of q was different. Therefore, we concluded that the discontinuity observed in these blends corresponds to the ODT but not the LDOT. The discontinuity indicates that the sharp first and higher order peaks and hence the long range order of the domain structure disappear with increasing temperature, leading to a broader, weaker first-order peak only. Furthermore, the discontinuity indirectly indicates that the interface between the PS and PI blocks in the material also disappears,[19] and thus that the discontinuity reflects the ODT into the disordered state where the PS and PI chains are molecularly mixed with some thermal composition fluctuations.

In Figures 3 and 4, we show a plot of the domain spacing as a function of temperature. Here it should be emphasized that, surprisingly enough, only a few works[36] have reported the domain spacing D as a function of temperature over a wide range of temperatures across ODT for blends of block copolymers and homopolymers, although a quite number of works have reported it for pure block copolymers. There are some works which report D as a function of blend composition for blends of block copolymers and homopolymers.[37] Error bars here correspond to $\pm^1/_2$ of the channel width of the detector.[38] Furthermore, for the 0.60 and 0.54 volume fraction diblock blends (Figure 4) there is a discontinuity in the domain spacing at the ODT temperature.[39] The 0.36 and 0.44 volume fraction blends show a slope change when the temperature of the sample is close to the glass transition temperature. Finally, except for the 0.71 volume fraction diblock blend the domain spacing consistently increases with increasing volume fraction homopolymer.

An ODT temperature indicated by a discontinuity in I_m^{-1} or σ_q^2 vs $1/T$ for the 0.44 and 0.36 volume fraction

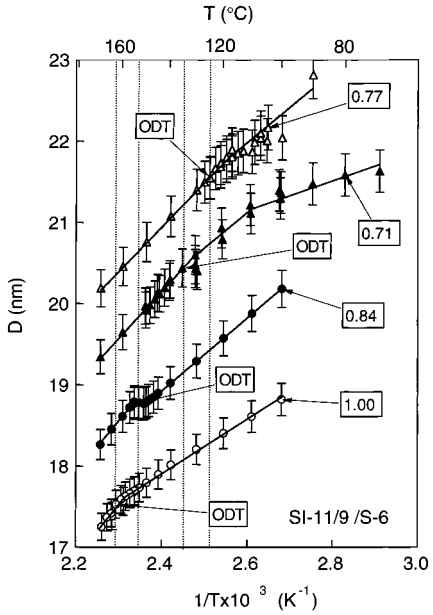

Figure 3. D vs $1/T$ for pure SI-11/9 (○) and SI-11/9/S-6 blends with compositions 0.84/0.16 (v/v) (●), 0.77/0.23 (v/v) (△), and 0.71/0.29 (v/v) (▲). Lines through points are to guide the eye. Vertical dotted lines indicate the ODT temperatures as determined from Figure 1.

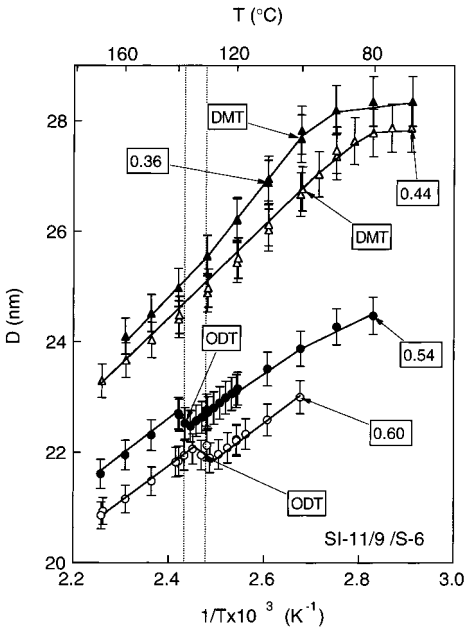

Figure 4. D vs $1/T$ for SI-11/9/S-6 blends with compositions 0.60/0.40 (v/v) (○); 0.54/0.66 (v/v) (●), 0.44/0.56 (v/v) (△), and 0.36/0.64 (v/v) (▲). Lines through points are to guide the eye. Vertical dotted lines indicate ODT temperatures as determined from Figure 2.

diblock blends is not seen from the plot of I_m^{-1} or σ_q^2 vs $1/T$ in Figure 2. Instead, in these two samples, the DMT temperature[32] was discerned by the disappearance of the form factor peak with increasing temperature. As an example, in Figure 5, we plot the scattering behavior of the 0.44/0.56 (v/v) blend as a function of temperature. At lower temperatures, there is a broad peak at $q/q_m \approx 3$ due to the form factor from spherical domains (90 and 100 °C) indicated by a fat arrow. Above 100 °C, the form factor peak effectively disappears as seen in scattering curve obtained at 110 °C. The highest temperature at which the form factor peak is apparent is considered to

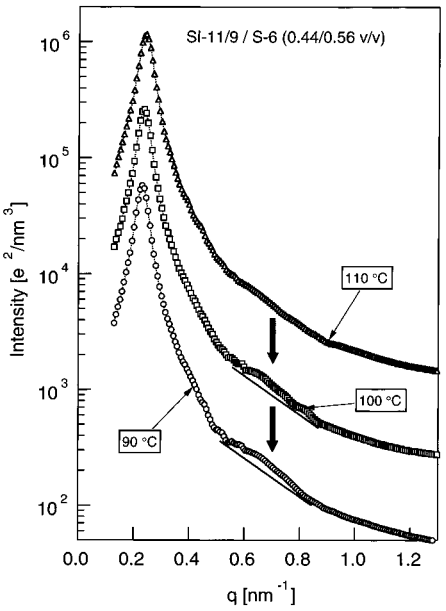

Figure 5. SAXS profiles at various temperatures showing the disappearance of the form factor peak with increasing temperature for SI-11/9 blended with S-6 (0.44/0.56 v/v): 90 °C (○); 100 °C (□); 110 °C (△). Successive curves are shifted down by a factor of 5 for clarity.

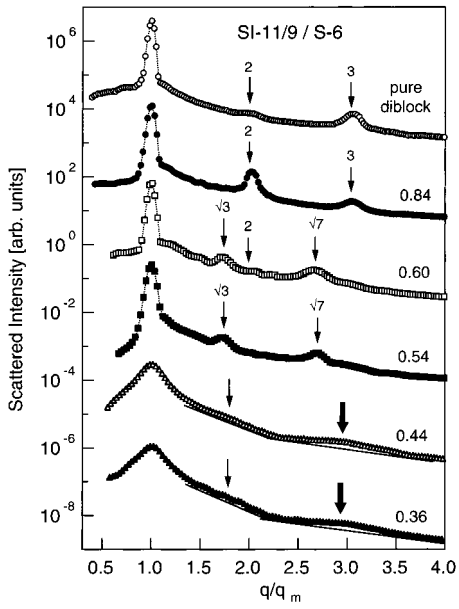

Figure 6. SAXS intensity against normalized scattering vector q/q_m for pure SI-11/9 and SI-11/9 blended with S-6 at various compositions after long annealing: pure diblock SI-11/9 (○); 0.84/0.16 v/v blend (●); 0.60/0.40 v/v blend (□); 0.54/0.46 v/v blend (■); 0.44/0.56 v/v blend (△); 0.36/0.64 v/v blend (▲). Numbers next to each scattering profile indicate the volume fraction of diblock copolymer SI-11/9. Successive curves are shifted down by a factor of 50 for clarity.

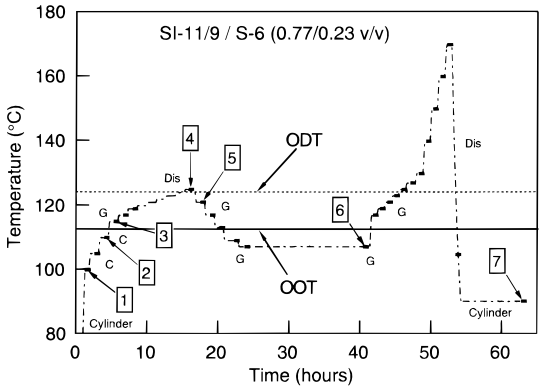

Figure 7. Thermal history for OOT measurement of SI-11/9/S-6 blend, 0.77/0.23 (v/v). Numbers correspond to scattering profiles in Figure 8.

be the temperature corresponding to the onset of demicellization (dissolution of the spherical domains themselves), and the lowest temperature at which the form factor peak is clearly not existing is considered to be the temperature corresponding to the completion of demicellization. This is a microphase transition from a spherical domain system with an interface but no long-range order to a disordered system with no interface and no order: the transition from spheres (or nanocolloidal particles) of PI in a PS matrix (with an interface) to disordered SI (no interface). Similar behavior is observed for the 0.36 volume fraction diblock blend.

At this point, we should point out that the temperature width over which the order−disorder transition occurs in the heating cycle was usually as broad as we cared to measure it. We can consider the measured temperature width of the ODT as the difference in temperature between the last temperature clearly showing order (onset of disordering) and the first temperature clearly showing disorder (completion of disordering). For example in the 0.84/0.16 v/v blend of SI-11/9 with S-6, the last datum showing only ordered phase is 151 °C and the first datum showing only disordered phase is 155 °C (see Figure 1). The intermediate point corresponds to 153 °C. Thus, the measured width of the transition is about 4 °C and the ODT is chosen as 153 °C in this work, intermediate between 151 and 155 °C. The width of the ODT transition is probably overestimated, and the apparent width of the ODT depends on the temperature resolution of the measurement. This criterion is used to make the error bars in Figure 10, which will be discussed later. If we measure in 3 deg steps, the width of the transition was 6 deg and if we measure in 2 deg steps, the width of the transition was usually 4 deg. That is, there usually was one data point intermediate between order and disorder. This intermediate data point suggests that the ODT may have a finite width but that width is still very small.

3.2. Structure Determination in the Ordered State. The classical ordered structures of SI diblock copolymer systems are well established for pure diblock copolymers[23] and blends of diblock copolymers/homopolymers.[24] Therefore, to determine the structure of these blends of interest here, we used both the results of SAXS measurements and expectations based on previously reported experimental studies on the effect of overall Φ_{PS} on structure as described in the Introduction.[23,24]

Figure 6 is a plot of the scattered intensity as a function of reduced scattering vector, q/q_m, for blends in the SI 11/9/S-6 system to show the microdomain structure of each blend in the ordered state. To ensure the presence of higher angle scattering peaks, some samples were annealed overnight at about 100 °C (above the glass transition temperature, but below the ODT temperature) to create larger grains and a better ordered structure. Since we observe known diblock copolymer structures whose structure is well established, only the first two or three peaks are used for structure identification. The pure diblock and first blend (0.84 volume fraction diblock) have peaks at positions

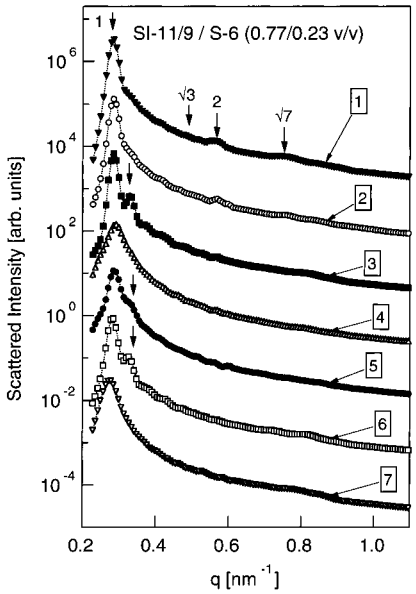

Figure 8. SAXS profiles for SI-11/9 blended with S-6 (0.77/0.23 v/v): 100 °C (▼, profile 1); 110 °C (○, profile 2); 115 °C (■, profile 3); 125 °C (△, profile 4); 121 °C (●, profile 5); 107 °C after 10 h annealing (□, profile 6); 90 °C (▽, profile 7). Successive curves are shifted down by a factor of 20 for clarity.

of q_m, $2q_m$, and $3q_m$, (indicated by thin arrows) which indicate a lamella structure. The second order peak of the pure SI-11/9 is weak due to the nearly 50/50 volume ratio of PS and PI lamellae in the pure block. The 0.77 and 0.71 volume fraction diblock copolymer blends will be discussed in the next section due to the complex order−order transition (OOT) these materials show. The 0.60 and 0.54 volume fraction diblock blends show peaks at q_m, $\sqrt{3}q_m$, and $\sqrt{7}q_m$. This scattering pattern suggests either a cylindrical structure on a hexagonal lattice or spherical structure on a body-centered cubic (bcc) lattice microdomain structure. However, previous reports[23,24] showing that these blend compositions are expected to show cylindrical structure, along with the absence of a $\sqrt{2}q_m$ peak cause us to assign a cylindrical structure to these two blends. Finally, the 0.44 and 0.36 volume fraction diblock blends have a first-order scattering peak and a broad form factor peak. The form factor for each blend is indicated by a fat arrow. Therefore, these two blends seem to have formed spherical microdomains showing liquidlike order. These results except for the 0.77 and 0.71 volume fraction diblock copolymer blends are consistent with structures reported elsewhere for SI diblock copolymer/PS homopolymer blend systems.[23,24]

To check if the 0.44 and 0.36 volume fraction diblock blends would show an ordered lattice, the 0.44 volume fraction diblock blend was annealed overnight at 100 °C. The results, which, in fact, is the one shown in Figure 6, show that a lattice did not form. Careful inspection of the scattering curves reveals that there is a broad, weak second peak (indicated by a thin arrow) or shoulder. However, such a peak could also arise in a system of spheres packed with liquidlike order.[40,41] Other reports have examined the transition from ordered spheres to disordered spheres (an LDT or LDOT (lattice disordering/ordering transition)) and then on to disorder (demicellization transition).[32−34] In our case, the lattice ordering from disordered spheres to ordered spheres is below the T_g of these materials and is therefore inaccessible.

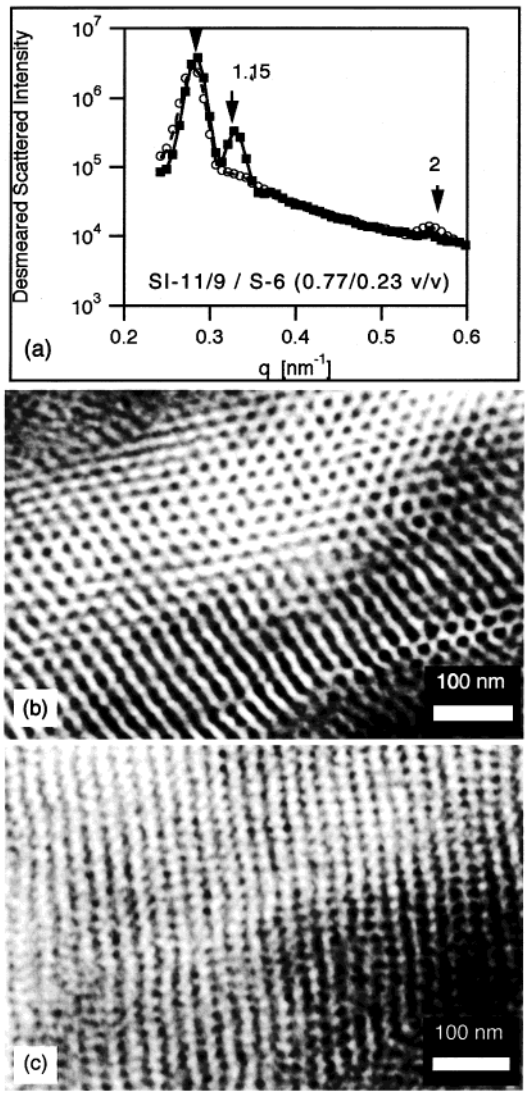

Figure 9. Transmission electron micrographs confirming cylinder and gyroid structures, before and after OOT, with SAXS data, SI-11/9 blended with S-6 (0.77/0.23 v/v): (a) SAXS profiles for samples having cylindrical structure (○) and gyroid structure (■); (b) TEM of samples having cylindrical structure and (c) gyroid structure.

3.3. Order−Order Transition. A large number of works have been devoted to and reported on the temperature-induced order−order transition (OOT) for pure diblock copolymers.[26,42−48] However, the temperature-induced OOT in diblock copolymer/homopolymer blends has been suggested experimentally for only one system: [49] the transition from lamella to gyroid. Therefore, the studies along this line are still quite new and insufficient. The direct in situ observation of the OOT is especially important in establishing the universality of the OOT, which has been observed in pure diblocks[50] and diblock copolymer/diblock copolymer blends.[51−54] Below, we discuss the observation of the temperature-induced order−order transition in the SI-11/9/S-6 blend system with 0.77 and 0.71 volume fraction of diblock.

In this experiment, the observation of the OOT was dependent on the thermal history of the sample. Three distinct processes were identified: slow heating, slow cooling, and fast cooling. Each of these processes led to a distinct structural change. Slow heating gave a transition from cylinder to gyroid (OOT) and then to disordered phase, slow cooling, a transition from disor-

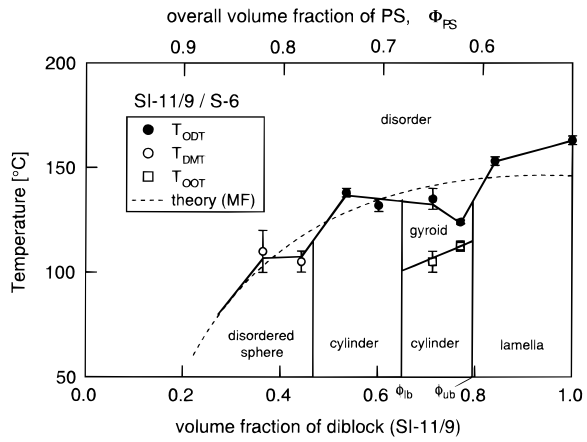

Figure 10. T_{ODT} (●), T_{DMT} (○), and T_{OOT}(□) vs volume fraction diblock in SI-11/9/S-6 blend. Vertical lines separating microdomain structures are obtained from the total volume fraction PS in the system and other reports on the effect of volume fraction PS on the microdomain structure. The dashed line indicates the results of a mean field calculation for ODT. Error bars are described in text. Note that the OOT line which exists at volume fractions PS between ϕ_{lb} and ϕ_{ub} was obtained during a heating process. A slow cooling from the disordered melt gave gyroid phase at all temperatures below the ODT temperature, while a rapid cooling below the OOT temperature gave cylinder phase which were stable at least for 10 h upon annealing at temperatures above T_g but below the OOT temperature.

dered phase to gyroid (ODT) and no further OOT, and fast cooling, a transition from disordered phase to cylinder (ODT), as detailed below. In addition, we consider a long annealing process of gyroid, formed during the slow cooling process, at temperatures for the low-temperature cylinder phase, which was expected to show a transition from gyroid to cylinder. However, it did not. This is similar to the results of Forster et al.[46] on a pure block copolymer system who observed that the gyroid phase showed pronounced metastability.

The thermal history of a sequence of measurements is shown in Figure 7. The thick horizontal lines represent the times during which SAXS profiles were measured (20 min). Prior to this measurement a cylindrical structure was formed by fast cooling. At first, the sample was heated in steps to identify the transition from cylinders to gyroid (slow heating, points 1−3). Then, the sample was cooled in steps to form gyroid (point 5) from disorder (point 4) and then cooled further in an attempt to form cylinders (point 6). Finally, the sample was heated again to well above the ODT and then cooled quickly to form cylinders (fast cooling, point 7), completing the cycle. Scattering profiles corresponding to the numbered points in Figure 7 are discussed below.

Figure 8 shows the scattering profiles in the heating and cooling cycle corresponding to the points in Figure 7. At low temperatures (profiles 1 and 2) in the heating cycle, a cylindrical structure is observed, indicated by peaks at q_m, $2q_m$, and $\sqrt{7}q_m$, but there is no side peak at $1.15q_m$, which would indicate gyroid structure. These structure assignments are supported by TEM evidence, which is described later (Figure 9). On heating the blend, one obtains a series of SAXS profiles that show no side peak, but at over 110 °C, the SAXS profile shows a second peak at $1.15q_m$ as shown by the arrow (profile 3), indicative of a bicontinuous gyroid structure, is obtained. Finally, on further heating, we obtain a profile with only a single broad peak which indicates disorder (profile 4) and corresponds to point 4 in Figure 7. This series of scattering profiles indicates an OOT from cylinders to gyroid and an ODT from gyroid to the disordered phase.

We should emphasize that the side peaks observed in the plots shown correspond to either shoulders or peaks in the original, smeared X-ray data and are not an artifact of the desmearing process. Also, the ODT from gyroid to disorder is still marked by a dramatic change in I_m^{-1} and σ_q^2 as a function of $1/T$ as shown in Figure 1 (see the data for the 0.77 and 0.71 diblock blend).

Next, let us consider the slow cooling process. Here, we begin with a disordered sample (point 4 in Figure 7). On cooling, we obtain a profile 5 showing a side peak (at point 5). This is indicative of a transition from disorder to gyroid. To check to see if one can observe a transition from gyroid to cylinder, the sample was cooled further, then annealed for a long time (12 h) at 107 °C to point 6 in Figure 7. From the scattering pattern (profile 6) corresponding to point 6, shown in Figure 8, we see here that the long annealing does not lead to a cylindrical structure, as the side peak is clearly still present.

Finally, let us consider the fast cooling cycle, necessary to obtain the cylindrical structure. We heat the blend well above the ODT temperature (i.e., to 170 °C), followed by cooling to 90 °C, below the ODT temperature of 124 °C (point 7 in Figure 7) over a relatively short period of about 1.5 h. In this case, we observe a sharp first-order scattering peak. Again, no side peak was observed (profile 7 in Figure 8). The first order peak is broader than usual, probably due to the relatively fast cooling to near or below T_g of the PS matrix. The sample corresponding to profile 1 was prepared in the same way. Profiles 1 and 7 differ due to the different thermal history of each sample, leading to a better defined structure for profile 1. After profile 7, the sample was measured again for the TEM (described below), and the microdomain structure was confirmed to be cylindrical.

In summary, on heating the sample with cylindrical microdomain structure slowly, we observe an OOT from cylinders to gyroids where the OOT temperature exists between 110 and 115 °C. On cooling the sample slowly from the disordered phase, a gyroid structure is formed. However, on further cooling below the OOT temperature between gyroid and cylinder, the cylindrical structure is not obtained. When the blend is quickly cooled from a temperature above the ODT to a temperature below the OOT temperature, however, the cylindrical structure is obtained. There seems to be a large kinetic barrier to the formation of cylindrical structure from gyroid, while the reverse proceeds normally. Consistent with our results, Hajduk et al. also observed that the transition from gyroid to lamella is kinetically limited.[49]

To check our interpretation of the X-ray scattering results which only had a limited number of scattering peaks, we conducted real-space observation by TEM. In parts b and c of Figure 9 we show the results of TEM observation. Figure 9a shows the SAXS profiles corresponding to the micrographs in Figure 9, parts b and c. First, a sample with alleged cylindrical structure was prepared by fast cooling. Namely, a blend specimen with 0.77 volume fraction of diblock was quickly cooled from above the ODT temperature to 100 °C which is below the OOT temperature, annealed at 100 °C for several hours to make well-ordered structures, and quenched to room temperature. To ensure that the quenching did

not change the structure, we measured the X-ray scattering profile both before and after the quench and the SAXS profiles before and after quenching were nearly the same, indicating that the quenching process did not change the structure. The SAXS profile thus obtained is shown in Figure 9a (open circles). Then, some of the sample was removed and microtomed for examination by transmission electron microscopy (TEM), the results of which are shown in Figure 9b. From this micrograph, one can observe cylinders on a hexagonal lattice, confirming our interpretation of the X-ray data above in Figure 9a (open circles) and the profiles 1, 2, and 7 in Figure 8.

After the sample for TEM was removed to check the cylindrical structure, the remaining sample was then returned to the X-ray instrument and annealed to form a gyroid structure by slowly raising the temperature (from room temperature) to above the OOT temperature, but below the ODT temperature, and quenched again. Again, the final structure before and after quenching was checked by SAXS. The SAXS results indicated that the structure showed no change. The SAXS pattern obtained this way has the clear side peak as shown in Figure 9a with filled squares. This sample was then microtomed and examined by TEM, as shown in Figure 9c. From this micrograph, one can observe a gyroid structure, which confirms our interpretation of the SAXS patterns.

Because this in situ observation of an OOT is unusual, as a further check, we performed in situ SAXS measurements on a sample with a similar blend composition: 0.71 volume fraction diblock. Similar behavior appears; that is, a fast cooling of the blend from the disordered phase leads to cylindrical structure, and a slow heating of this specimen, a transition from cylinder to gyroid. We do not show the SAXS profiles for this blend, since the trend observed in the change of the SAXS profiles accompanied by the structure transformation is similar to that observed for the blend with 0.77 volume fraction diblock. Here, the OOT seems to appear at between 100 and 110 °C. In this sample the side peak was much less pronounced than in the 0.77 volume fraction SI-11/9/S-6 blend. From this measurement, we show that the OOT is reproducible.

It is noteworthy that at the OOT a discontinuity in I_m^{-1} or σ_q^2 vs $1/T$ is not observed for the instrument resolution used in the present SAXS experiment. This could be due to insufficient temperature resolution during the measurement, or due to the difficulty in discerning a difference in peak height and width for such sharp peaks from the ordered structure due to finite beam width smearing effects.

From the in situ scattering profiles as a function of temperature for two blends, we know that these blends undergo an OOT. TEM evidence, from one sample, confirms the structure assignments from the X-ray data. Finally, as shown previously in section 3.1, the ODT can be clearly identified by a discontinuity in a plot of I_m^{-1} or σ_q^2 vs $1/T$.

4. Discussion

4.1. Domain Spacing *D*. The need for investigation of D as a function of temperature was pointed already in section 3.1. Increasing temperature leads to smaller values of D as seen in Figures 3 and 4. This is due to the fact that as the temperature increases, the net repulsive interactions between the PS and PI weaken,[6] allowing a larger interface area per unit volume. Also, the addition of homopolymer leads to larger values of D by swelling the PS domains to a larger degree than the decreasing values of D due to increasing the interfacial area per SI junction at the interface between lamellar layers.[55] Since the PS homopolymer has a shorter chain length than the PS block of the block copolymer, these materials are known to show so-called "wet-brush" behavior.[56] This means that the PS homopolymer is dissolved in the PS block of the block copolymer, spreading the junctions and increasing the interfacial area as well as the domain spacing.

Some of the domain spacing vs $1/T$ plots shown in Figures 3 and 4 show a large change in the slope of the plot of D vs $1/T$. This change occurs at temperatures close to the T_g of polystyrene, suggesting that this slope change at the low-temperature range is linked to the glass transition of these materials.

4.2. Order−Disorder Transition. The unique point of this work on the phase diagram of the ODT was already pointed out in section 1. In Figure 10, we show the effect of blend composition on the ODT for the blend. The figure also shows the results of mean-field calculations for blends. For this blend, we used $\chi = -0.073 + 50/T$ where T is the absolute temperature. This equation was derived from the ODT data with the assumption that the mean field theory[4] is valid. That is, the value of χ at the ODT (χ_{ODT}) for each composition was calculated from the random phase approximation, and then, the constants A and B for the calculation of χ_{ODT} from T using the relation $\chi = A + B/T$ were chosen such that the measured T_{ODT} had the same χ_{ODT} value as the results from the calculation. Thus, the calculated curve has two adjustable parameters, appearing in the calculation of temperature from the theoretically predicted value of χ. Here, we see that the addition of homopolymer decreases the ODT temperature for the nearly symmetric diblock copolymer. The mean-field theory predicts this trend. Thus, the mean-field theory remains a reasonable model from the point of view that it qualitatively predicts the composition dependence of the ODT.

The data shown in Figure 10 reflect the lowest ODT temperature ($T_{ODT,L}$, lower temperature limit for the error bars) and the highest ODT temperature ($T_{ODT,U}$, upper temperature limit for the error bars). The data point marking the ODT is intermediate between these two values. Thus, the ODT should be regarded as within the range of the error bars given, and not necessarily at the point drawn. It should also be noted here that the transition points for the 0.36 and 0.4 volume fraction diblock blends refer to T_{DMT} (demicellization/micellization transition temperatures)[32] rather than T_{ODT} for blends with other compositions.

Comparison of the phase diagram obtained here with those of other workers brings out some intriguing points. It is striking to note that there is an anomalous drop in ODT for one blend composition (0.77 volume fraction diblock). However, other works, although on pure diblock copolymers, have also reported similar behavior,[48] a drop in the ODT at one particular volume fraction polystyrene in a polystyrene-*block*-poly(2-vinylpyridine) copolymer as well as in PS−PI block copolymers.[26] Here the drop of ODT appears to be coupled, as will be discussed below, with the temperature-induced order−order transition (OOT) and/or complex morphology like gyroid or hexagonal perforated layers (HPL)

Table 2. Characteristics of the Blends Studied

composition of SI block copolymer		ODT temperature		OOT temperature		
wt fract	vol fract	$T_{ODT,U}$[a] (°C)	$T_{ODT,L}$[b] (°C)	$T_{OOT,U}$[e] (°C)	$T_{OOT,L}$[f] (°C)	structure in ordered phase
1	1	165	161			lamella
0.83	0.84	151	155			lamella
0.76	0.77	125	123	115	110	cylinder gyroid
0.70	0.71	140	130	110	100	cylinder gyroid
0.59	0.60	135	129			cylinder
0.52	0.54	140	136			cylinder
0.43	0.44	110[c]	100[d]			disordered spheres
0.35	0.36	120[c]	100[d]			disordered spheres

[a] Highest ODT temperature. [b] Lowest ODT temperature. [c] Highest DMT (micellization/demicellization transition) temperature instead of $T_{ODT,U}$. [d] Lowest DMT temperature instead of $T_{ODT,L}$. [e] Lowest temperature showing gyroid structure only. [f] Highest temperature showing cylindrical structure only.

existing immediately below ODT in both block copolymer/homopolymer blends and pure block copolymers. Thus, we discuss here OOT in conjunction with ODT, although we separately discuss OOT itself in next section.

Schultz et al. observe the drop of ODT accompanied by the temperature-induced OOT from hexagonal perforated layers (HPL) to gyroid.[48] In addition, for a polyisoprene-*block*-polystyrene diblock copolymer, at high volume fractions of PS, a decrease in the ODT temperature is also observed, along with the OOT from gyroid to HPL.[26] Therefore, we see common features in all three systems: the OOT and a drop in the ODT temperature at compositions close to those where the OOT is observed. In contrast to the studies of pure block copolymers, in the blend system studied here, the OOT is a transition from cylinders to gyroid instead of HPL to gyroid or gyroid to HPL. It was shown later that the HPL structure is metastable and transformed to gyroid on annealing.[57] If this is the case, these two pure block copolymer systems turned out not to show the OOT. Thus, the drop of ODT turns out to be associated with the gyroid morphology in the case of the pure block copolymers.

This anomalous drop in the ODT temperature at about 0.77 volume fraction diblock corresponds to the gyroid phase. This fact may suggest that the gyroid phase, regardless of whether the systems are pure block copolymer systems or blend systems, is not as stable as other type of ordered phases. It may also suggest that the gyroid phase at a shallow quench below ODT is formed very slowly and hence appears disordered or still contains many defects with the time scale of our observation. Thus, the intriguing drop of ODT should be further studied in future.

4.3. Order−Order Transition (OOT). Some unique points of this work on OOT were already pointed out in section 3.3. In the phase diagram shown in Figure 10, we took the OOT observed in the slow heating process as being the range where we last see the cylindrical phase without coexistence of the gyroid phase (lower temperature limit of the error bar, $T_{OOT,L}$) to where we first see the gyroid phase without coexistence of the cylindrical phase (upper temperature limit of the error bar, $T_{OOT,U}$). It should be stressed that a part of the phase diagram in Figure 10 with volume fraction of diblock ϕ_b from ϕ_{lb} to ϕ_{ub} which involves temperature-induced OOT was obtained in the heating process on the specimens prepared by rapidly cooling from disordered state. As already indicated in section 3.3, the slow cooling of the blends with $\phi_{lb} \leq \phi_b \leq \phi_{ub}$ from disordered state showed only the gyroid phase below T_{ODT}, while the rapid cooling of the blends from disordered state showed the cylinder phase at temperatures below T_{OOT}.

The domain structures as a function of volume fraction of one component polymer (e.g., PS) observed here are consistent with those observed by others [23,24] for a broad range of SI diblock copolymer systems. Therefore, the data of Hasegawa et al. [23] and Winey et al.[24] are used to draw vertical lines separating different structures in Figure 10. Also, we observe a temperature-induced OOT at two blend compositions, and therefore, it is clearly shown to be a reproducible phenomenon in this diblock copolymer/homopolymer blend system. The only single work previously reported on SI block copolymer/homopolystyrene or polyisoprene blend[49] revealed a thermoreversible temperature-induced OOT between lamella and gyroid, while the present work revealed a temperature-induced OOT between cylinder and gyroid which is not reversible. The difference may be attributed to difference in molecular weight and composition of the block copolymers used and the molecular weights of the homopolymers used. Thus, the present work contributes to information regarding the OOT in the block copolymer/homopolymer blends.

Let us next compare the OOT in the present work with the OOT concerning a transition between gyroid and cylinders reported for pure SI block copolymers.[26,46] The latter works on the pure block copolymers did not even investigate the thermoreversibility of the OOTs. The unusual feature of the present work is that cylinders are the *low*-temperature phase, while in ref 26, which is concerned with the SI rich in polyisoprene block, they are the *high*-temperature phase. However in defense of the present work, ref 46, which is concerned with the SI rich in polystyrene block, also finds the OOT from cylinders to gyroid transition on heating. These observations are intriguing and may provide fundamental information concerning similarity and dissimilarity between pure block copolymers and block copolymers/homopolymer blends, although correct interpretations are still unclear.

We believe the thermoirreversibility of the OOT between cylinder and gyroid is due to a kinetic effect as discussed in section 3.3. The transformation from a simple symmetry to a complex symmetry occurs much faster than the transformation from a complex symmetry to a simple symmetry as in the case of the OOT between hexagonally packed cylinders and spheres packed in body-center-cubic lattice[50] and the OOT between lamellae and gyroids.[57] The transformation from cylinders to gyroids may occur much faster than the transformation from gyroids to cylinders. Thus, in

the time scale of our observation, we found the cylinder-to-gyroid transition but not the gyroid-to-cylinder transition. The gyroid, which is formed at temperatures between ODT and OOT, is kinetically trapped even below OOT where cylinders are expected to be formed. The *low*-temperature cylinder phase may be formed in the time scale of our observation only when we avoid formation of gyroid through quickly cooling the melts to temperatures below OOT. Upon quick cooling of the disordered melts to a given temperature between ODT and OOT, the blends are initially disordered but eventually ordered into gyroids indicating that the *high*-temperature gyroid phase is at least thermally at equilibrium.

It might be plausible that the cylinders formed after a rapid quench are kinetically favored but thermodynamically unstable; in contrast, gyroids are kinetically unfavored but thermodynamically more stable than cylinders at the low-temperature range below T_{OOT}. Even in this case, we can explain our observation. We know the *low*-temperature cylinder phase is stable upon annealing above T_g of the polystyrene phase for at least 10 h, indicating that the above scenario is not likely. However, we need further prolonged annealing to rule out this scenario.

As in the case of pure diblock copolymers and diblock copolymer/diblock copolymer blends, the phase diagram is complex, showing order−order transitions as well as order−disorder transitions. All diblock copolymer systems—pure diblocks, blends of a diblock copolymer with homopolymer, and blends of diblock copolymers with other diblock copolymers—have similar behaviors. It is likely that the inclusion of fluctuation effects is also important in constructing a theoretical phase diagram due to the observed divergence between the theoretical and experimental results. A prediction of ODT from the ordered phase rather than the prediction of ODT from the disordered phase may also be important future work.

To facilitate comparison of these experimental data with theoretical efforts, we have listed the blend compositions and observed transitions in Table 2. We give ranges of temperatures to reflect the true uncertainties in these results.

5. Conclusions

Blends of diblock copolymers and homopolymers show complex phase behavior, and the phase diagram prepared using the more recent criterion for the ODT should be helpful in critically evaluating current theoretical efforts in the field as well as guiding expectations about the behavior of similar blend systems. Finally, the phase diagram shows that features seen in all diblock copolymer systems are universal: the ODT, the OOT, ordered structures, and spherical domains with short-range liquidlike order.

References and Notes

(1) Hashimoto, T. In *Thermoplastic Elastomers, A Comprehensive Review*; Legge, N. R.; Holden, G., Schroeder, H. E., Eds.; Hanser: Munich, Germany, 1996; p 429.
(2) Hasegawa, H.; Hashimoto, T. In *Comprehensive Polymer Science, Second Supplement*; Aggarwal, S. L., Russo, S., Eds.; Pergamon: New York, 1996; p 497.
(3) Leibler, L.; Benoit, H. *Polymer* **1981**, *22*, 195.
(4) Leibler, L. *Macromolecules* **1980**, *13*, 1602.
(5) Roe, R.-J.; Fishkis, M.; Chang, J. C. *Macromolecules* **1981**, *14*, 1091.
(6) Hashimoto, T.; Shibayama, M.; Kawai, H. *Macromolecules* **1983**, *16*, 1093.
(7) Zin, W.-C.; Roe, R.-J. *Macromolecules* **1984**, *17*, 183.
(8) Bates, F. S.; Hartney, M. A. *Macromolecules* **1985**, *18*, 2478.
(9) Hashimoto, T.; Ijichi; Fetters, L. J. *J. Chem. Phys.* **1988**, *89*, 2463.
(10) Ijichi, Y.; Hashimoto, T.; Fetters, L. J. *Macromolecules* **1989**, *22*, 2817.
(11) Roe, R.-J.; Zin, W. C. *Macromolecules* **1984**, *17*, 189.
(12) Nojima, S.; Roe, R.-J. *Macromolecules* **1987**, *20*, 1866.
(13) Fredrickson, G. H.; Helfand, E. *J. Chem. Phys.* **1987**, *87*, 697.
(14) Bates, F. S.; Rosedale, J. H.; Fredrickson, G. H. *J. Chem. Phys.* **1990**, *92*, 6255.
(15) Stühn, B.; Mutter, R.; Albrecht, T. *Europhys. Lett.* **1992**, *18*, 427.
(16) Wolff, T.; Burger, C.; Ruland, W. *Macromolecules* **1993**, *26*, 1707.
(17) Hashimoto, T.; Ogawa, T.; Han, C. D. *J. Phys. Soc. Jpn.* **1994**, *63*, 2206.
(18) Floudas, G.; Pakula, T.; Fischer, E. W.; Hadjiichristidis, N.; Pispas, S. *Acta Polym.* **1994**, *45*, 176.
(19) Sakamoto, N.; Hashimoto, T. *Macromolecules* **1995**, *28*, 6825.
(20) Ogawa, T.; Sakamoto, N.; Hashimoto, T.; Han, C. D.; Baek, D. M. *Macromolecules* **1996**, *29*, 2113.
(21) Bodycomb, J.; Yamaguchi, D.; Hashimoto, T. *Polym. J.* **1996**, *28*, 821.
(22) Yamaguchi, D.; Hashimoto, T.; Han, C. D.; Baek, D. M.; Kim, J. K.; Shi, A.-C. *Macromolecules* **1997**, *30*, 5832.
(23) Hasegawa, H.; Tanaka, H.; Yamasaki, K.; Hashimoto, T. *Macromolecules* **1987**, *20*, 1651.
(24) Winey, K. I.; Gobran, D. A.; Xu, Z.; Fetters, L. J.; Thomas, E. L. *Macromolecules* **1994**, *27*, 2392.
(25) Hajduk, D. A.; Harper, P. E.; Gruner, S. M.; Honeker, C. C.; Thomas, E. L.; Fetters, L. J. *Macromolecules* **1995**, *28*, 2570.
(26) Khandpur, A.; Forster, S.; Bates, F. S.; Hamley, I. W.; Ryan, A. J.; Bras, W.; Almdal, K.; Mortensen, K. *Macromolecules* **1995**, *28*, 8796.
(27) Suehiro, S.; Saijo, K.; Ohta, Y.; Hashimoto, T. *Anal. Chim. Acta* **1986**, *189*, 41.
(28) Fujimura, M.; Hashimoto, T.; Kawai, H. *Mem. Fac. Eng., Kyoto Univ.* **1981**, *43* (2), 224.
(29) Hashimoto, T.; Suehiro, S.; Shibayama, M.; Saijo, K.; Kawai, H. *Polym. J.* **1981**, *13*, 501.
(30) Burger, C.; Ruland, W.; Semenov, A. N. *Macromolecules* **1990**, *23*, 3339.
(31) Tanaka, H.; Hashimoto, T. *Polym. Commun.* **1988**, *29*, 212.
(32) Han, C. D.; Vaidya, N. Y.; Kim, D.; Shin, G.; Yamaguchi, D.; Hashimoto, T. *Macromolecules* **2000**, *33*, 3767.
(33) Sakamoto, N.; Hashimoto, T.; Han, C. D.; Kim, D.; Vaidya, N. Y. *Macromolecules* **1997**, *30*, 1621.
(34) Sakamoto, N.; Hashimoto, T.; Han, C. D.; Kim, D.; Vaidya, N. Y. *Macromolecules* **1997**, *30*, 5321.
(35) Above LDT, but below ODT, the system loses long-range order but still keeps its microdomain structure with a sharp interface.
(36) Tanaka, H.; Hashimoto, T. *Macromolecules* **1991**, *24*, 5713. Here most of the data were reported for blends of block copolymers and homopolymers with dioctyl phthalate to lower the ODT temperature to within the range of experimentally accessible temperatures.
(37) See for example, Hashimoto, T.; Tanaka, H.; Hasegawa, H. *Macromolecules* **1990**, *23*, 4378. Koizumi, S.; Hasegawa, H.; Hashimoto, T. *Makromol. Chem., Macromol. Symp.* **1992**, *62*, 75. Kimishima, K.; Hashimoto, T.; Han, C. D. *Macromolecules* **1995**, *28*, 3842.
(38) Curve-fitting results suggest that the error bars for the domain spacing are extremely small, much smaller than the symbols in Figures 3 and 4.
(39) While we note the discontinuity here, and note that it is reproducible, the absolute value of the discontinuous change is too small to measure accurately. However, this discontinuity merits further study. In the vicinity of the first-order scattering peak, the instrument we use has a q resolution of about 7×10^{-3} nm^{-1}. This corresponds to a change in domain spacing of about 0.3 nm, which is the same magnitude as the observed discontinuity. An instrument with about five times the angular resolution, corresponding to a resolution of about 1 arc second (about 10^{-3} nm^{-1}) such as a Bonse-Hart USAXS instrument would be able to more clearly discern the discontinuity as well as accurately measure the magnitude of the discontinuity.
(40) Kinning, D.; Thomas, E. L. *Macromolecules* **1984**, *17*, 1712.
(41) Kinning, D. J.; Thomas, E. L. *J. Chem. Phys.* **1989**, *90*, 5806.

(42) Almdal, K.; Koppi, K. A.; Bates, F. S.; Mortensen, K. *Macromolecules* **1992**, *25*, 1743.
(43) Sakurai, S.; Momii, T.; Taie, K.; Shibayama, M.; Nomura, S.; Hashimoto, T. *Macromolecules* **1993**, *26*, 485.
(44) Sakurai, S.; Kawada, H.; Hashimoto, T.; Fetters, L. *Macromolecules* **1993**, *26*, 5796.
(45) Hamley, I. W.; Koppi, K. A.; Rosedale, J. H.; Bates, F. S.; Almadal, K.; K.; M. *Macromolecules* **1993**, *26*, 5659.
(46) Forster, S.; Khandpur, A. K.; Zhao, J.; Bates, F. S.; Hamley, I. W.; Ryan, A. J.; Bras, W. *Macromolecules* **1994**, *27*, 6922.
(47) Hajduk, D. A.; Gruner, S. M.; Rangarajan, P.; Register, R. A.; Fetters, L. J.; Honeker, C.; Albalak, R. J.; Thomas, E. L. *Macromolecules* **1994**, *27*, 490.
(48) Schulz, M. F.; Khandpur, A. K.; Bates, F. S.; Almdal, K.; Mortensen, K.; Hajduk, D. A.; Gruner, S. M. *Macromolecules* **1996**, *29*, 2857.
(49) Hajduk, D. A.; Harper, P. E.; Gruner, S. M.; Honeker, C.; Kim, G.; Thomas, E. L.; Fetters, L. J. *Macromolecules* **1994**, *27*, 4063.
(50) Kimishima, K.; Koga, T.; Kanazawa, Y.; Hashimoto, T. *Scattering from Polymers, Characterization by X-rays, Neutrons, and Light*; ACS Symposium Series 739; American Chemical Society: Washington, DC, 2000; Chapter 32, p 514.
(51) Court, F.; Hashimoto, T. Manuscript in preparation.
(52) Court, F. These de Doctrat de l'Université Pierre et Marie Curie, 1996.
(53) Zhao, J.; Majumdar, B.; Schulz, M. F.; Bates, F. S.; Almdal, K.; Mortensen, K.; Hajduk, D. A.; Gruner, S. M. *Macromolecules* **1996**, *29*, 1204.
(54) Sakurai, S.; Irie, H.; Umeda, H.; Nomura, S.; Lee H. H.; Kim, J. K. *Macromolecules* **1998**, *31*, 336.
(55) Tanaka, H.; Hasegawa, H.; Hashimoto, T. *Macromolecules* **1991**, *24*, 240.
(56) Hashimoto, T.; Tanaka, H.; Hasegawa, H. *Macromolecules* **1990**, *23*, 4378.
(57) Hajduk, D. A.; Takenouchi, H.; Hillmyer, M. A.; Bates, F. S.; Vigild, M. E.; Almdal, K. *Macromolecules* **1997**, *30*, 3788.
(58) Inoue, T.; Soen, T.; Hashimoto, T.; Kawai, H. *J. Polym. Sci., Part A-2* **1969**, *7*, 1283.

MA9917996